

# 星形成ゼミ・報告 (SFN #310 N.55-58)資料

2018年12月7日

古屋 玲

(徳島大学・教養教育院)

---

## 紹介しない論文

55

EPIC 203868608: A low-mass quadruple star system in the Upper Scorpius OB association

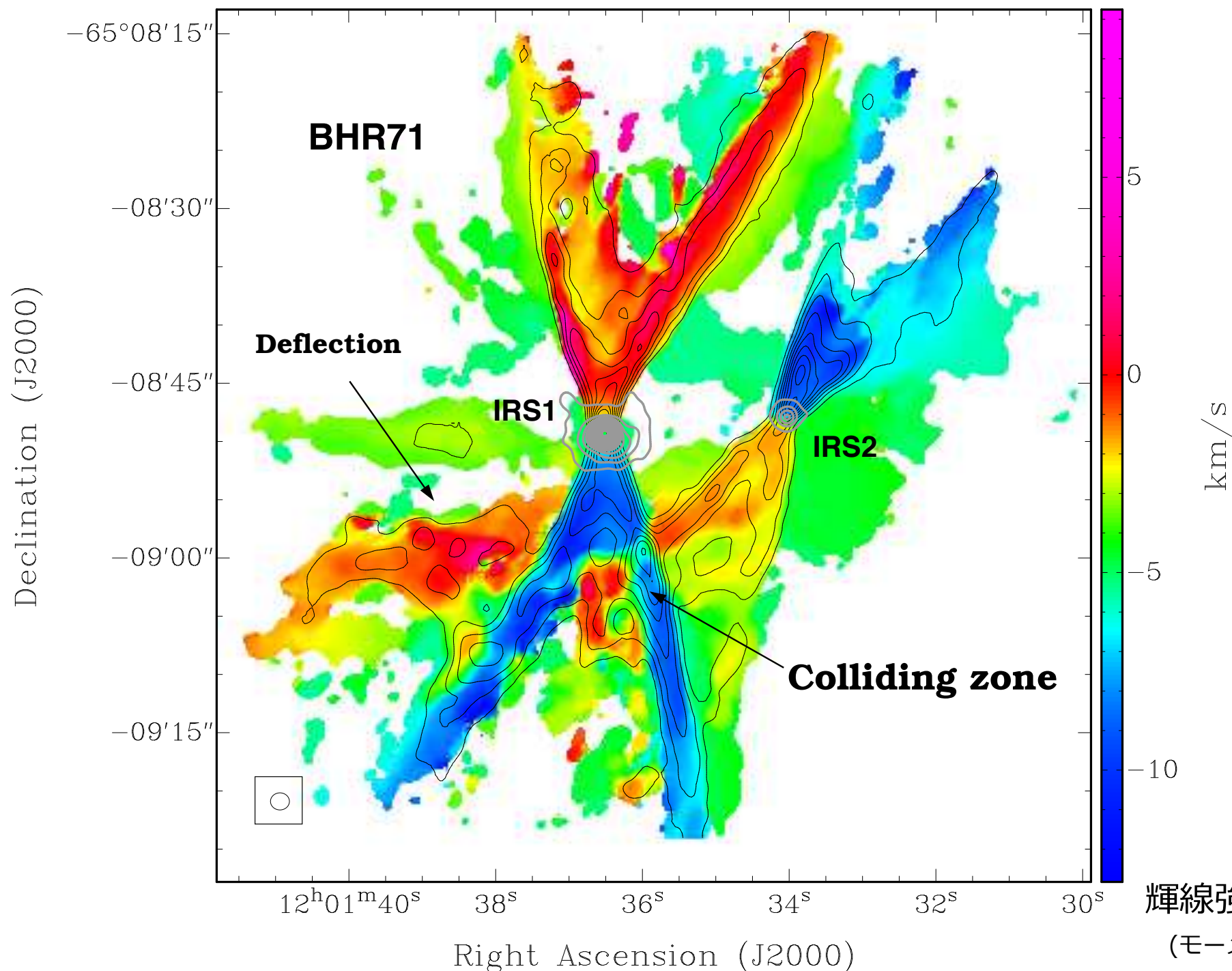
Ji Wang<sup>1,2</sup>, Trevor J. David<sup>1,3</sup>, Lynne Hillenbrand<sup>1</sup>, Dimitri Mawet<sup>1</sup>, Simon Albrecht<sup>4</sup>, and Zibo Liu<sup>5</sup>

## ALMA reveals a collision between protostellar outflows in BHR 71

Luis A. Zapata<sup>1</sup>, Manuel Fernández-López<sup>2</sup>, Luis F. Rodríguez<sup>1</sup>, Guido Garay<sup>3</sup>, Satoko Takahashi<sup>4</sup>, Chin-Fei Lee<sup>5</sup>, and Antonio Hernández-Gómez<sup>1,6</sup>

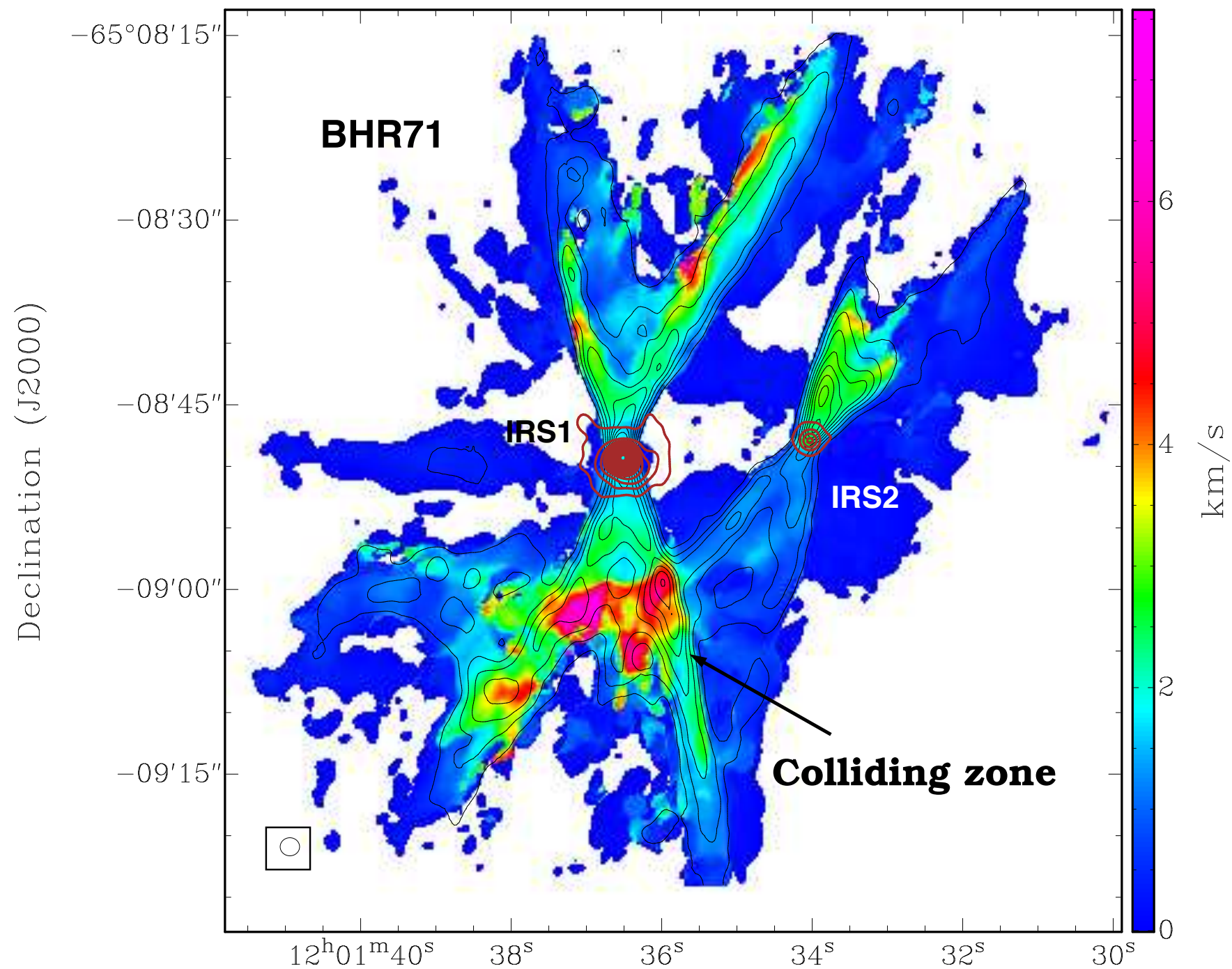
## 📌 要旨

1. 分子流と分子流が相互作用する系(3例目)をALMAでは初めて見つけた。
2. 【中心星のひとつ ; BHR71 IRS1】
  - $L_{\text{bol}} = 13.5 \pm 1.0 L_{\text{sun}}$
  - $M_{\text{dusty envelope}} = 0.215 \pm 0.003 M_{\text{sun}}(\text{ALMA}), 19 M_{\text{sun}}(\text{ハーシェル衛星})$
  - 分子流の力学年齢の下限値は,  
 GREG> say '200\*30\*au|(25e5)|yr'  
 1.1384E+03年くらい, second collapse後  
 それほど時間は経っていないか?



輝線強度で重み付け平均した視線速度マップ  
(モーメント計算時の速度範囲は  $-25 < V - V_{\text{sys}} \text{ (km/s)} < 20$ )

**Figure 2.** ALMA  $^{12}\text{CO}(2-1)$  intensity-weighted velocity (moment one) (color-scale),  $^{12}\text{CO}(2-1)$  integrated intensity (black contours), and 1.3 mm continuum (grey contours) images of BHR 71. The half-power synthesized beam size is shown in the bottom left corner. The radial velocity scale-bar is shown in the right. The black contours are starting from 10% to 80% in steps of 10% of the intensity peak. The CO intensity peak is  $13.9 \text{ Jy Beam}^{-1} \text{ Km s}^{-1}$ . The grey contours are starting from 2% to 90% in steps of 2% of the intensity peak. The 1.3 mm continuum intensity peak is  $0.4 \text{ Jy Beam}^{-1}$ .



Right Ascension (J2000) 輝線強度で重み付け平均した視線速度の速度幅マップ  
(モーメント計算時の速度範囲は  $-25 < V-V_{\text{sys}} \text{ (km/s)} < 20$ )

**Figure 3.** ALMA  $^{12}\text{CO}(2-1)$  intensity-weighted square root velocity (moment two) (color-scale),  $^{12}\text{CO}(2-1)$  integrated intensity (black contours), and 1.3 mm continuum (brown contours) images of BHR 71. The half-power synthesized beam size is shown in the bottom left corner. The radial velocity scale-bar is shown in the right. The black contours are starting from 10% to 80% in steps of 10% of the intensity peak. The CO intensity peak is  $13.9 \text{ Jy Beam}^{-1} \text{ Km s}^{-1}$ . The brown contours are starting from 2% to 90% in steps of 2% of the intensity peak. The 1.3 mm continuum intensity peak is  $0.4 \text{ Jy Beam}^{-1}$ .



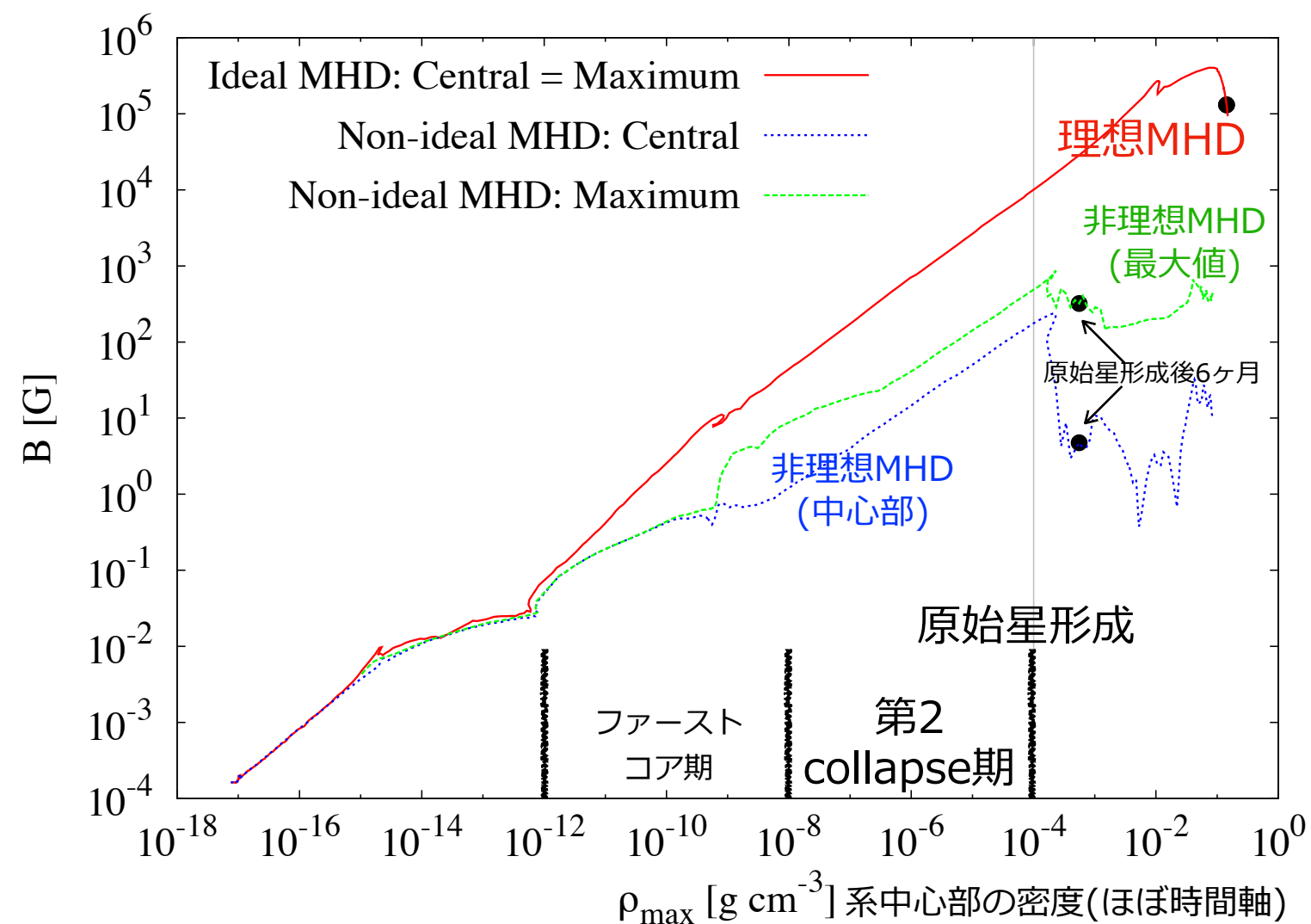


**Figure 1.** Evolution of the magnetic field strength against maximum density, which is a proxy for time. The vertical grey line indicates the formation density of the stellar core, and the black circles are placed 6 months after the formation of the stellar core for each model (i.e.  $dt_{sc} = 0.5$  yr). For both models, the maximum density is coincident with the centre of the system (i.e.  $\rho_{max} = \rho_{cen}$ ). In the ideal MHD model, the maximum and central magnetic field strength are the same for the entire simulation. In the non-ideal MHD model, the central and maximum magnetic field strengths are no longer coincident near the end of the first core phase, and at stellar core formation, are a few orders of magnitude lower than the values in the ideal MHD model.

1. 【着眼点】若い星[文脈から前主系列星 (PMS) ? ]で観測されるkGオーダーの磁場強度は原始星形成時にあったものか、それともPMS進化におけるダイナモで増幅されたものか？
2. 【手法】非理想MHD効果(双極性拡散, オーム損失, ホール効果)+回転を考慮し, 分子雲コア(初期に $R=0.013$ pc, 等温, 回転と重力のエネルギー比 $=0.005$ , 臨界値に対する質量磁束比 $\mu=5$ , 適切な宇宙線電離度 $\zeta=1e-17$  1/sec)から原始星形成直後までを計算.
3. 【結論】
  - (i)理想MHD(磁場と物質がカップル)では観測事実(?)を説明できない.
  - (ii)誕生直後の原始星は $r \sim 1-3$ AUの“magnetic wall”(図2参照)で囲まれており、壁での最大磁場強度は $\sim 900$ G, 中心星を含めた壁内部では $\sim 240$ G以下.
  - (iii)つまり, PMSで観測されるkGオーダーの磁場はPMS進化中に増幅されたものだろう.

【この論文と直接比較されている先行研究】

Tsukamoto+15a, 15b, 17

図3

$$\mu(r) \equiv \frac{M/\Phi_B}{(M/\Phi_B)_{\text{crit}}},$$

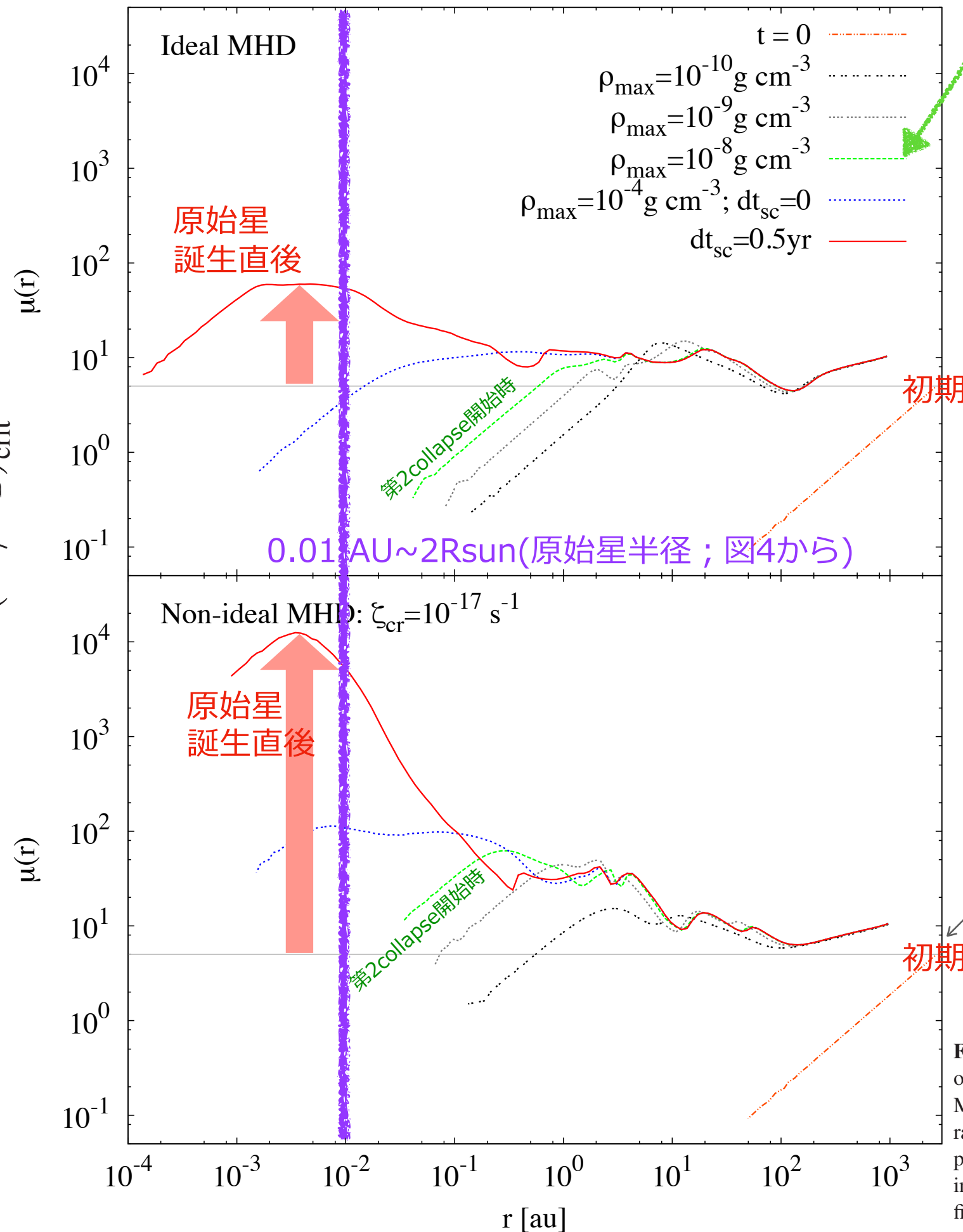


図2: ファーストコア期最終盤での磁場構造

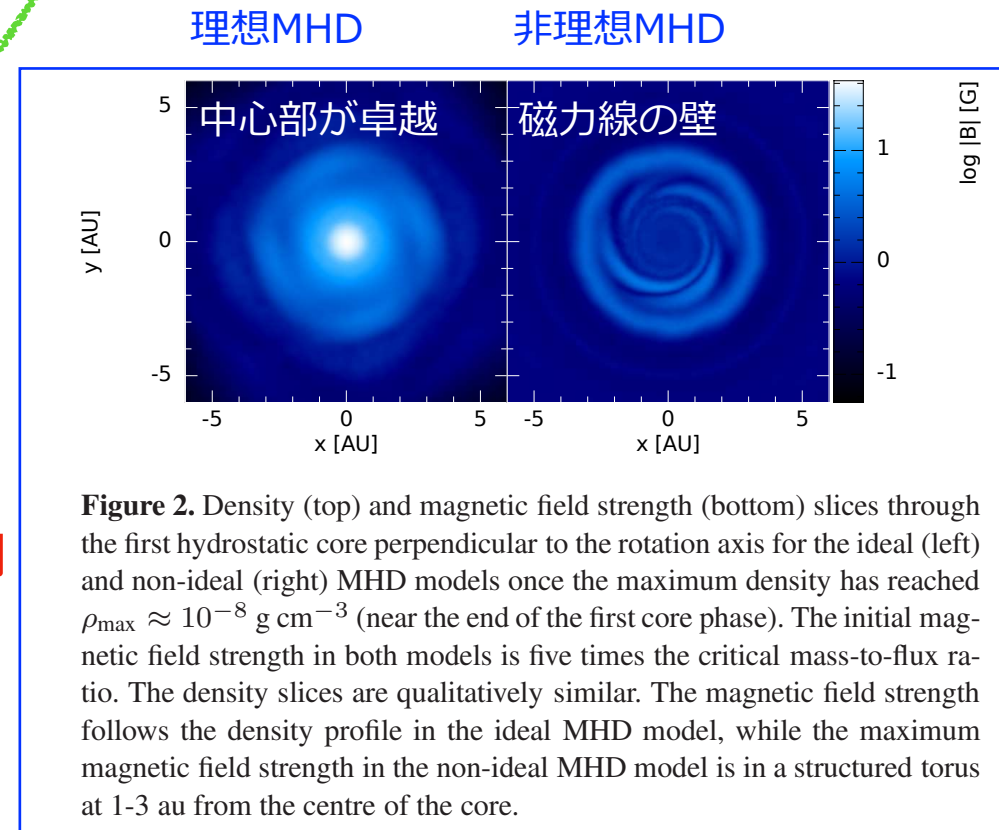


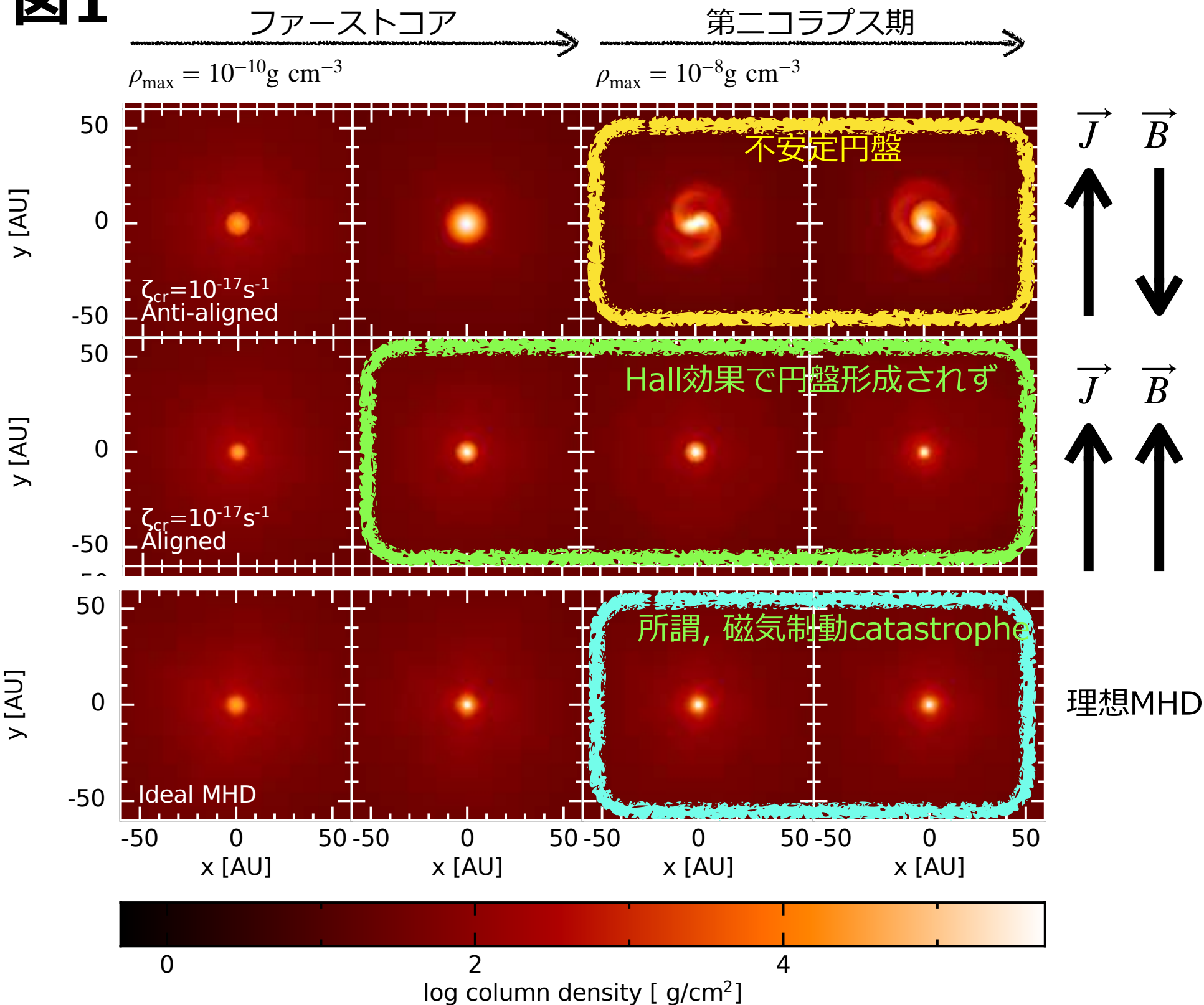
Figure 2. Density (top) and magnetic field strength (bottom) slices through the first hydrostatic core perpendicular to the rotation axis for the ideal (left) and non-ideal (right) MHD models once the maximum density has reached  $\rho_{\text{max}} \approx 10^{-8} \text{ g cm}^{-3}$  (near the end of the first core phase). The initial magnetic field strength in both models is five times the critical mass-to-flux ratio. The density slices are qualitatively similar. The magnetic field strength follows the density profile in the ideal MHD model, while the maximum magnetic field strength in the non-ideal MHD model is in a structured torus at 1-3 au from the centre of the core.

$$\mu = \frac{M/\Phi_B}{(M/\Phi_B)_{\text{crit}}} = \frac{\frac{M(r)}{\pi r^2 B(r)}}{\frac{c1}{3\pi} \sqrt{\frac{5}{G}}} \simeq$$

GREG> say 'Msun|(pi\*(0.013\*pc)\*\*2\*163e-6)|((.53|(3\*pi)\*sqrt(5|G)))'  
4.987

Figure 3. The mass-to-flux ratio in units of the critical value as a function of radius at six different epochs for the ideal (top) and non-ideal (bottom) MHD models. The horizontal grey line represents the initial mass-to-flux ratio,  $\mu_0 = 5$ . At  $t = 0$ ,  $\mu(r) = \mu_0 = 5$  at  $r = R_c$ . The non-ideal MHD processes diffuse the magnetic field even by  $\rho_{\text{max}} \approx 10^{-10} \text{ g cm}^{-3}$ , yielding  $\mu_{\text{non-ideal}}(r) > \mu_{\text{ideal}}(r)$ . There is significant diffusion of the magnetic field for  $r \lesssim 10 \text{ au}$  in the non-ideal MHD model.

## 図1



## 📌 要旨

1. 55番論文の結果のうち、不安定な円盤の形成に焦点
2. 【新しさ】 非理想MHD効果3つを入れて、分子雲コアから前主系列段階(のうち、ごく)最初まで、角運動量ベクトル $\vec{J}$ と磁場ベクトル $\vec{B}$ が平行と反平行の場合を解いた.
3. 【結果】
  - (i)図1の 部分で $r \sim 25 \text{ AU}$ の円盤形成されるので、所謂、磁気制動catastropheの問題を解決.
  - (ii)ファーストコア段階で分子流が駆動される.
    - 反平行のとき低速( $< 0.3 \text{ km/s}$ )分子流
    - 平行のとき高速( $> 3 \text{ km/s}$ )分子流

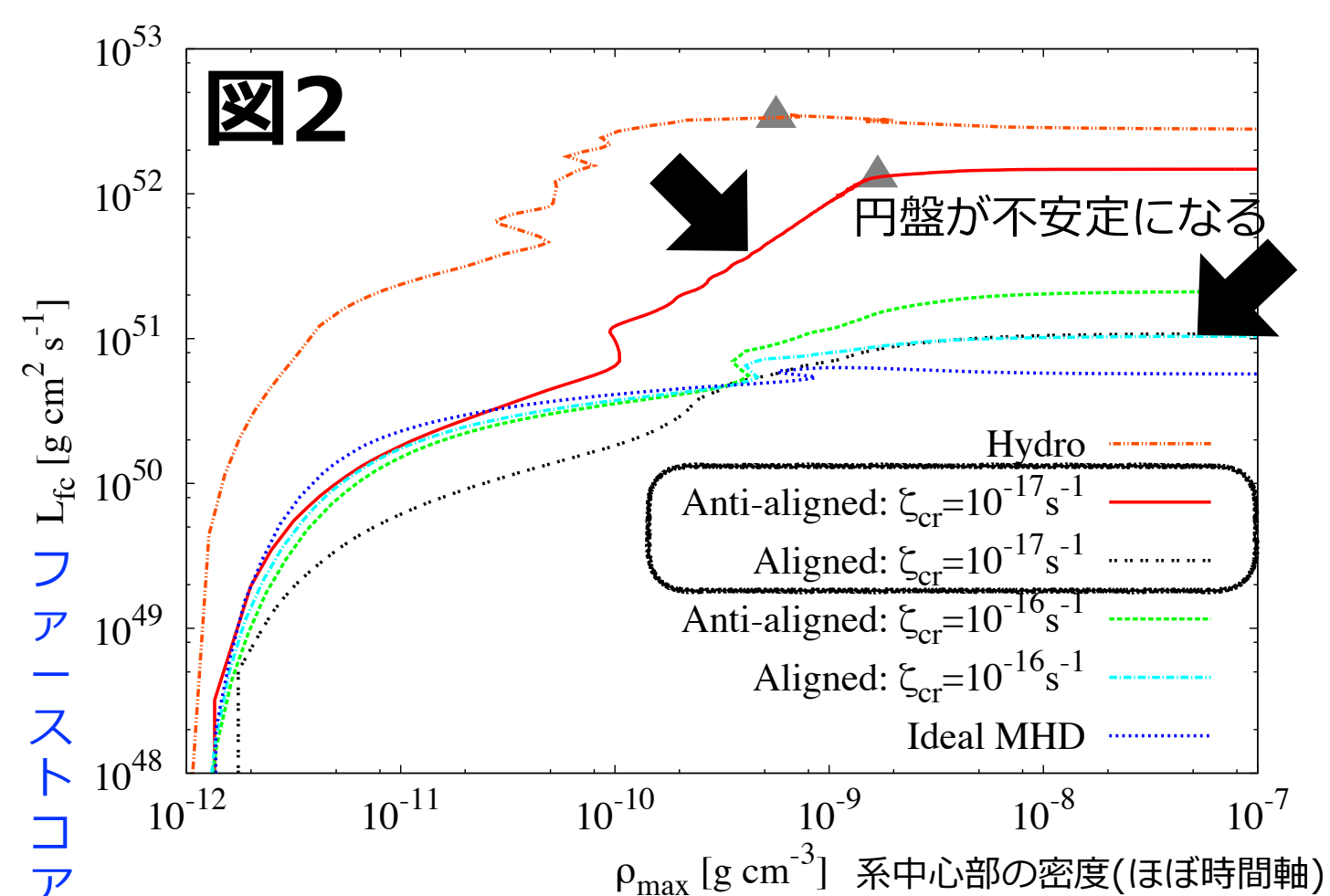


**Figure 2.** Evolution of the angular momentum in the first hydrostatic core (defined as the gas with  $\rho \geq 10^{-12} g cm^{-3}$ ). The triangles represent when the discs becomes gravitationally unstable. The angular momentum in the first core is larger for models with lower ionization rates, and with initially anti-aligned magnetic field and rotation vectors.

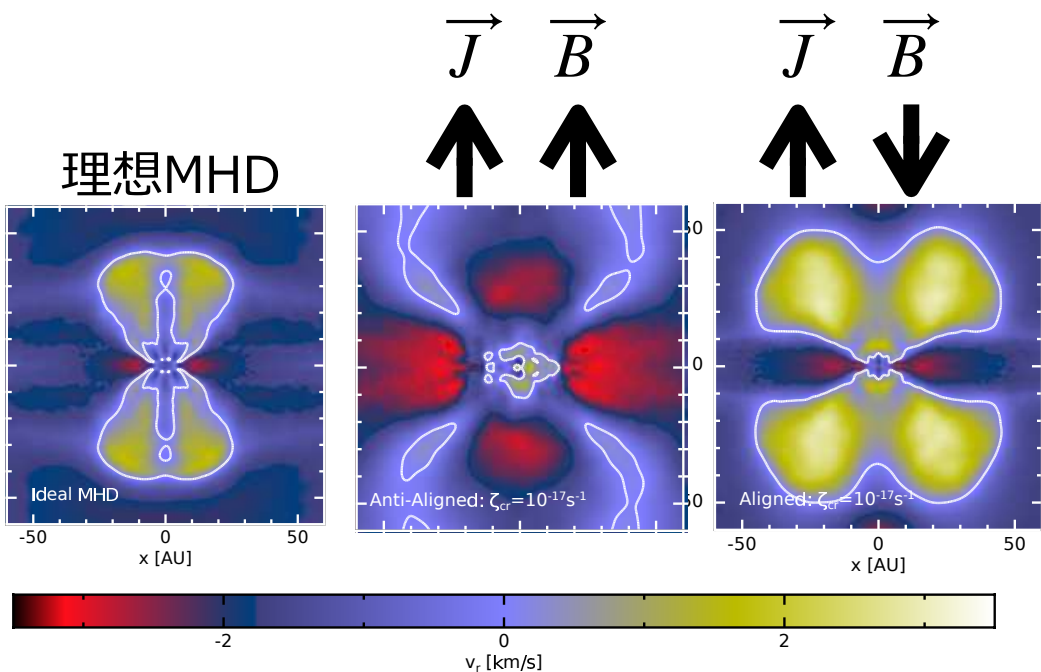
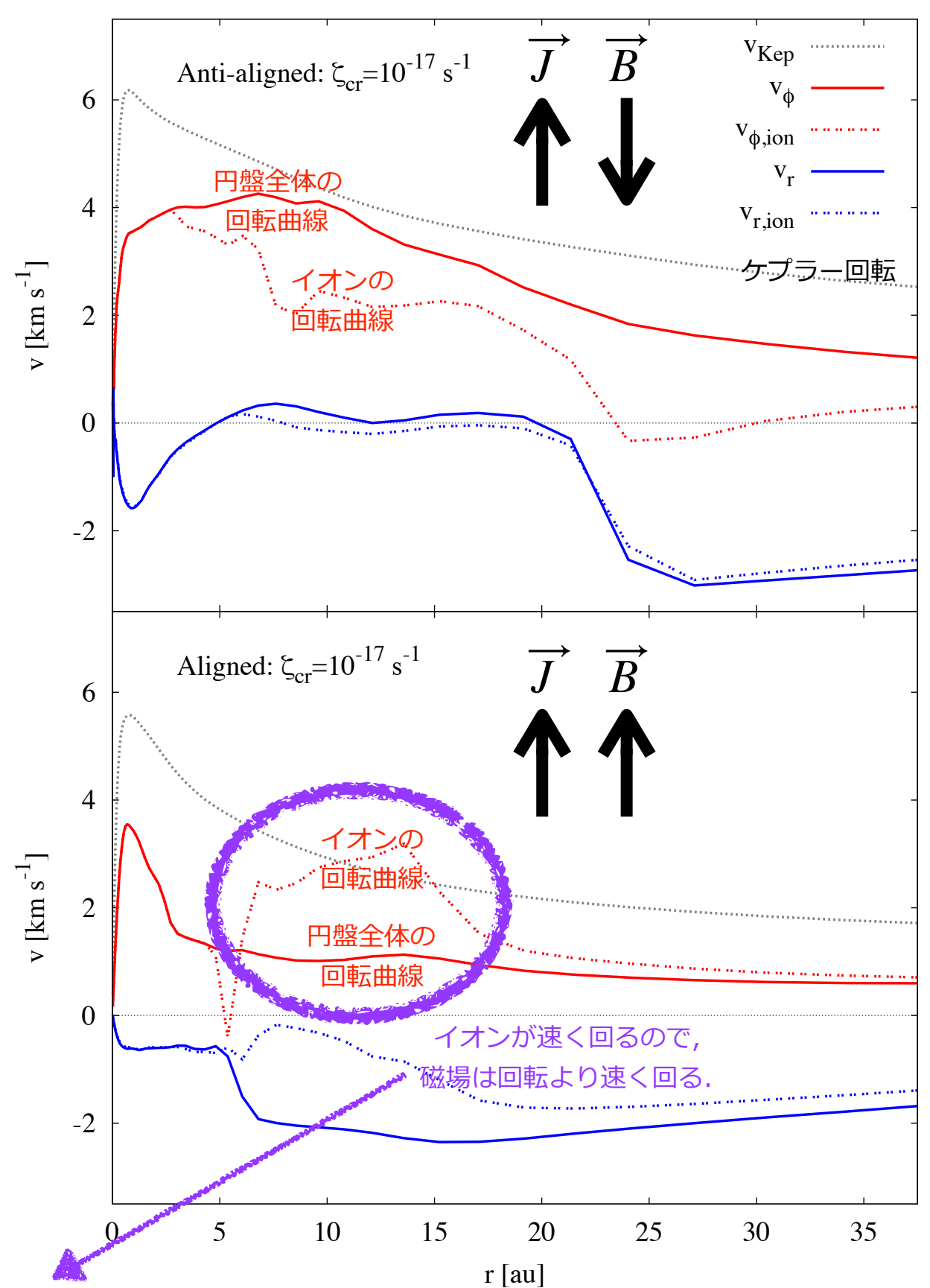


**図9: 分子流速度の視線成分**



より顕著なトロイダル磁場をつくる。

**Figure 3.** Azimuthally averaged single-fluid and ion velocities within 20° of the midplane at  $\rho_{max} \approx 10^{-7} g cm^{-3}$  for models  $\zeta_{17}^-$  (top) and  $\zeta_{17}^+$  (bottom). The gas is rotating at sub-Keplerian velocities. The ions are rotating slower than the bulk rotational flow in  $\zeta_{17}^-$ , decreasing the magnetic braking and promoting disc formation.